Science Advances

AAAS

advances.sciencemag.org/cgi/content/full/4/5/eaap9660/DC1

Supplementary Materials for

A cerebellar adaptation to uncertain inputs

Andrei Khilkevich, Jose Canton-Josh, Evan DeLord, Michael D. Mauk

Published 30 May 2018, *Sci. Adv.* **4**, eaap9660 (2018)
DOI: 10.1126/sciadv.aap9660

This PDF file includes:

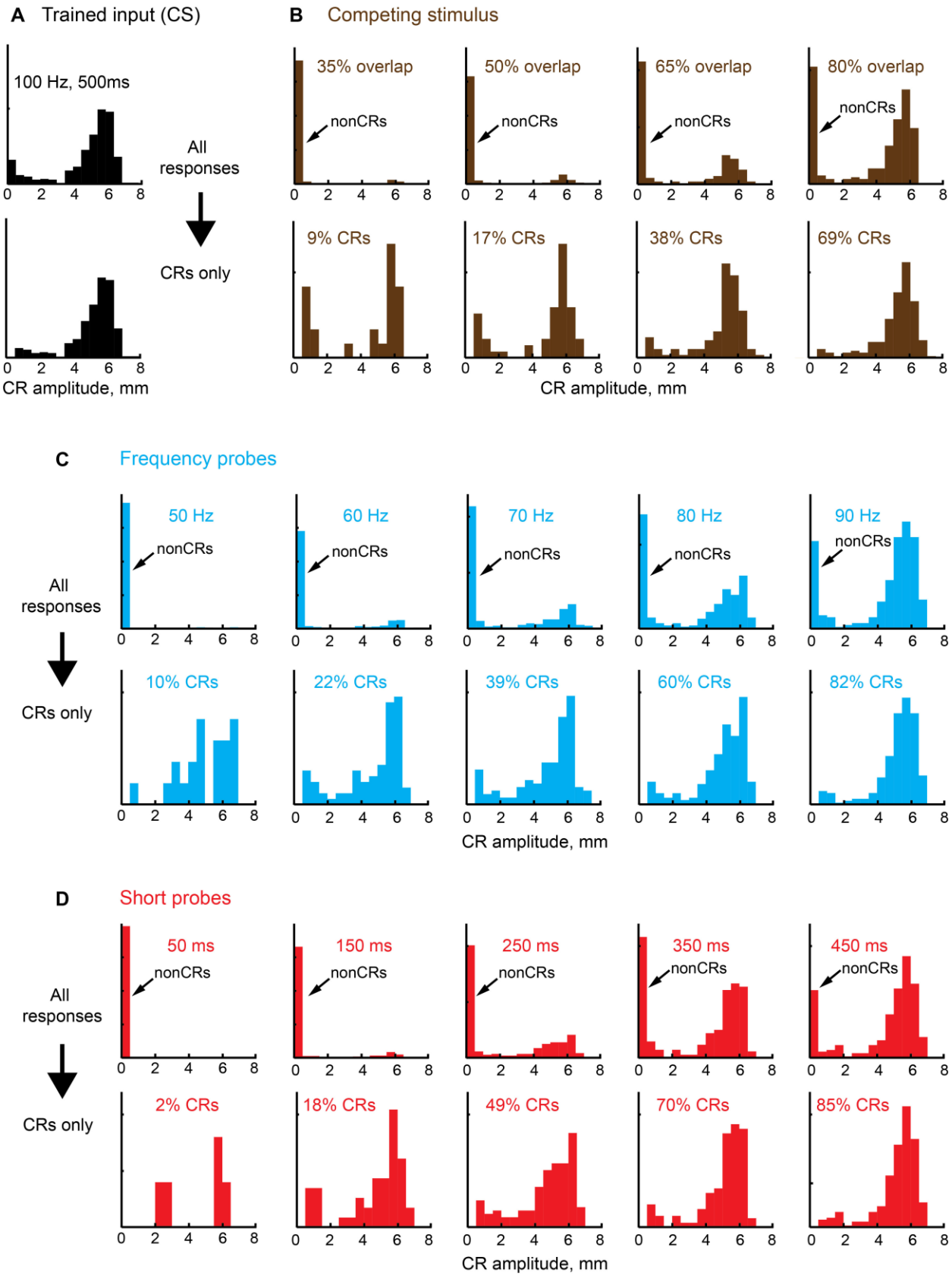
A Trained input (CS)
100 Hz, 500ms
All responses
CRs only
CR amplitude, mm
B Competing stimulus
35% overlap
50% overlap
65% overlap
80% overlap
nonCRs
9% CRs
17% CRs
38% CRs
69% CRs
CR amplitude, mm
C Frequency probes
50 Hz
60 Hz
70 Hz
80 Hz
90 Hz
10% CRs
22% CRs
39% CRs
60% CRs
82% CRs
CR amplitude, mm
D Short probes
50 ms
150 ms
250 ms
350 ms
450 ms
2% CRs
18% CRs
49% CRs
70% CRs
85% CRs
CR amplitude, mm

fig. S1. Distributions of CR amplitudes in response to different stimuli presentations. In all cases the top panels show distributions of all response amplitudes, while bottom panels show distributions of CR amplitudes only from trials with CRs present (0.5 mm cutoff). Data are shown from subjects trained to produce a full sized CR. The binary choice hypothesis predicts that CR amplitudes distributions in response to different probes should be statistically indistinguishable from responses to trained input after non-CRs are subtracted. (**A**) Distributions of CR amplitudes in response to trained input. (**B**) Responses to competing stimulus probes, with probe type and corresponding CR probability indicated in the legend. (**C**) The same layout for frequency probes. (**D**) The same layout for short probes. In all cases, distributions of all responses (shown on top) are clearly bimodal, with the first mode corresponding to nonCRs and second to trained full sized CR (around 6mm). After subtraction of nonCRs, distributions (on the bottom) are very similar to each other, despite changes in probe protocol, probe type and corresponding CR probability.

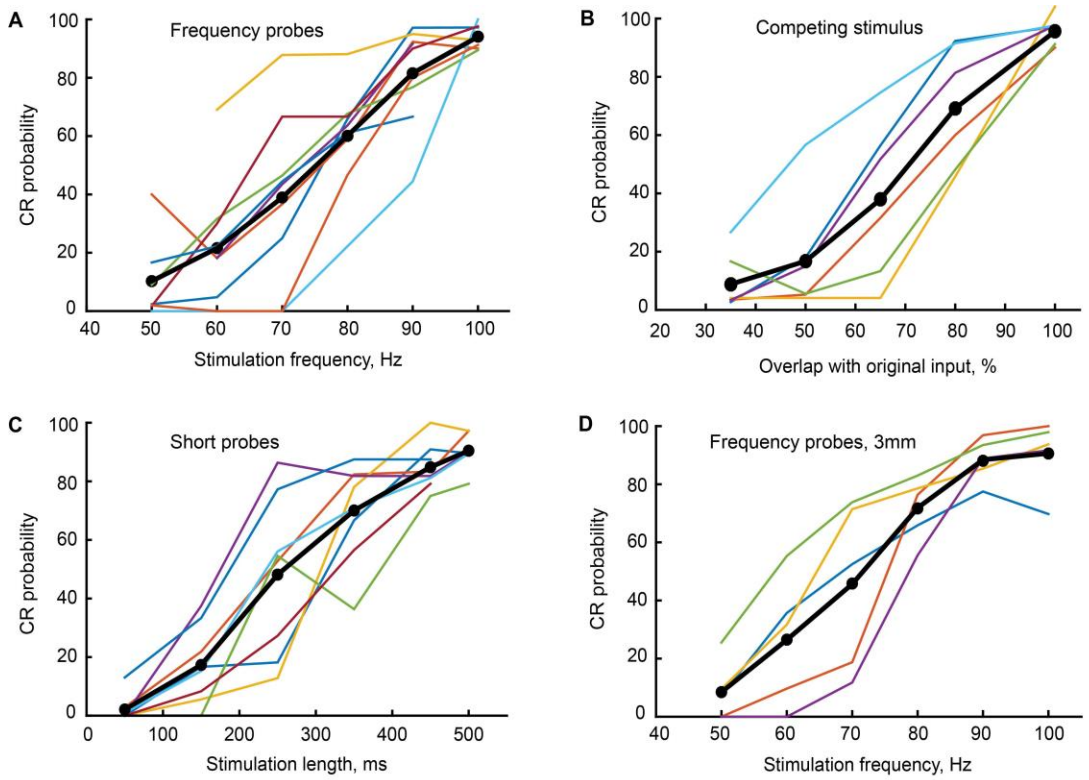

fig. S2. CR probability as a function of probe. Colored lines are shown separately for each rabbit, black line shows the average across subjects. Trained input corresponds to the most right point on X axis. The same color across panels does not necessary correspond to the same animal. (**A**-**C**) Data from subjects trained to produce a full sized (6mm) CR and then tested using either frequency probes, competing stimulus or short probes protocols, respectively. (**D**) Data from subjects trained to produce half-sized (3mm) CR and tested with frequency probes.

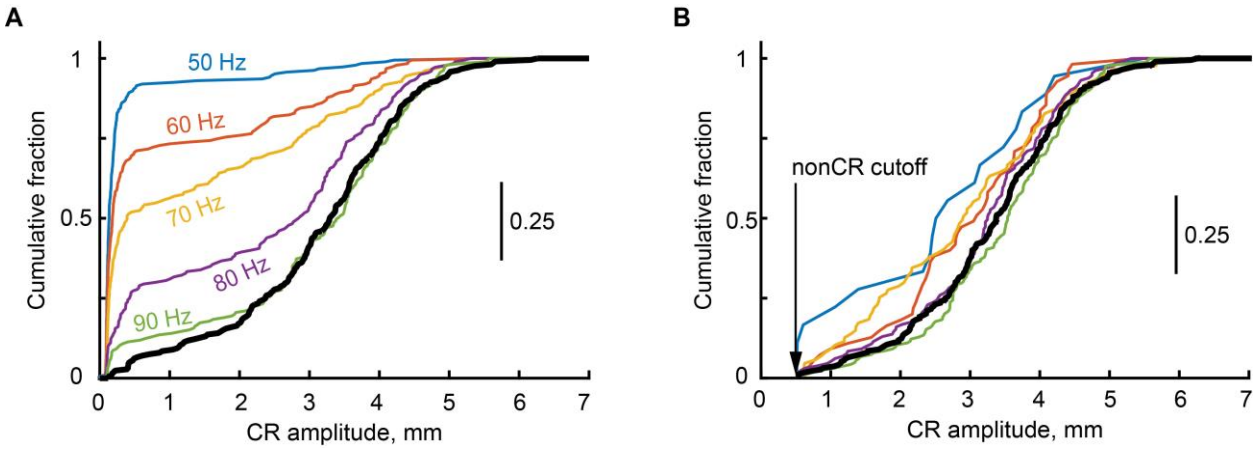

fig. S3. CDF of CR amplitudes for subjects trained to produce half-sized CRs. (**A**) CDF of all response amplitudes to frequency probes from subjects trained to produce a half-sized CR. Black line corresponds to CDF of responses to trained input. (**B**) Recolored from Fig. 2. F for illustrative purposes. The same as A, but with non-CRs subtracted from distributions.

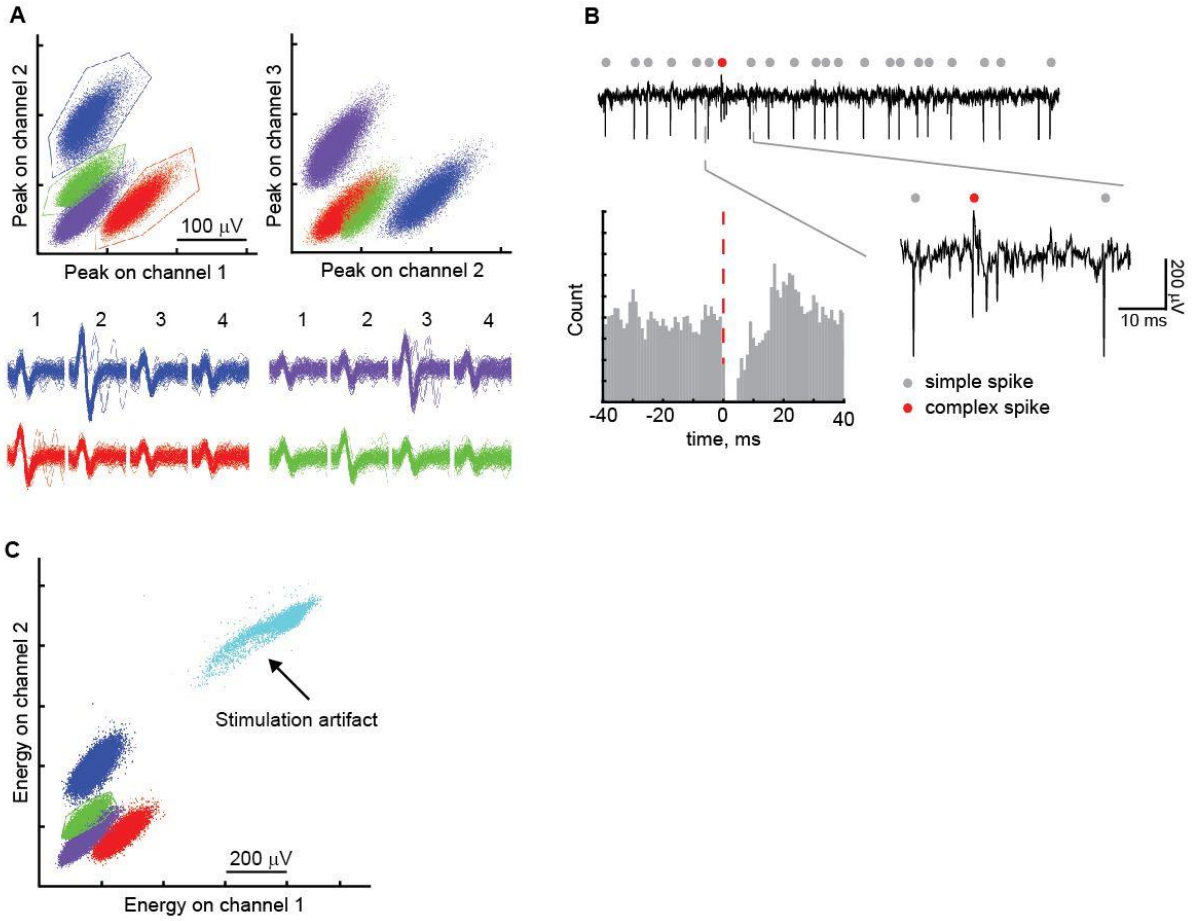

fig. S4. Isolation of single units and eyelid PCs from tetrode recordings. (**A**) Two top panels show four isolated single units in two cluster-cutting projections (peak on tetrode's channel 2 versus channel 1 and peak on channel 3 versus channel 2). A hundred of overlaid waveforms from each unit (color-coded) recorded on each channel is shown at the bottom. (**B**) Example continuous recording from a tetrode's channel with an eyelid PC. Grey dots indicate times of simple spikes, red dots indicated complex spikes. Times of simple and complex spikes were found from cluster-cutting procedure. A zoomed in portion with simple and complex spike waveforms is shown on the right. Spike-triggered average of simple spikes on complex spikes is shown on the left, demonstrating a post complex spike pause. (**C**) Cluster-cutting projection using energy parameter. Artifacts caused by electrical stimulation of mossy fibers (cyan cluster) are reliably isolated from single units.

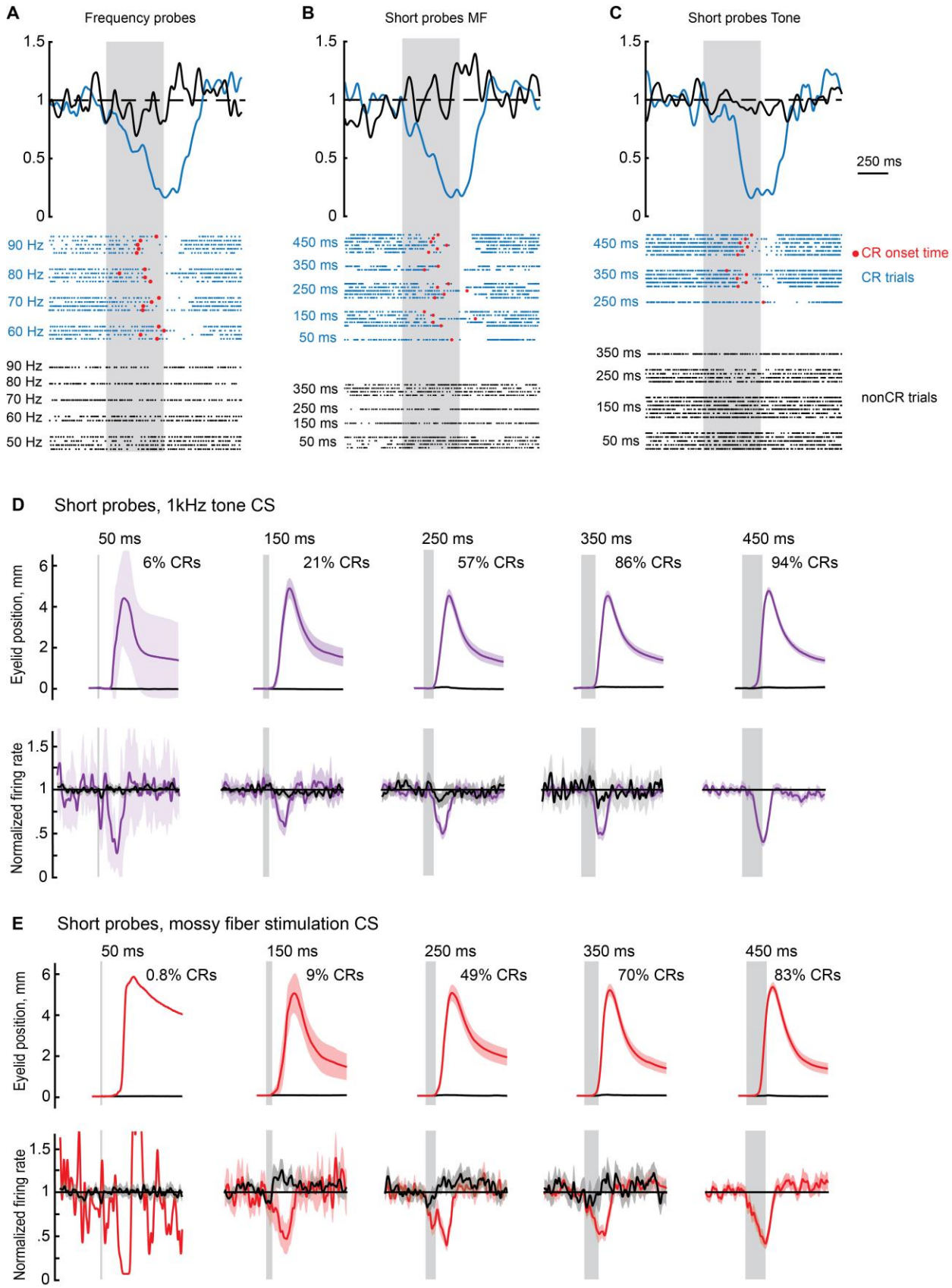
A
Frequency probes
B
Short probes MF
C
Short probes Tone
250 ms
CR onset time
CR trials
nonCR trials
90 Hz
80 Hz
70 Hz
60 Hz
50 Hz
450 ms
350 ms
250 ms
150 ms
50 ms
D
Short probes, 1kHz tone CS
6% CRs
21% CRs
57% CRs
86% CRs
94% CRs
Eyelid position, mm
Normalized firing rate
E
Short probes, mossy fiber stimulation CS
0.8% CRs
9% CRs
49% CRs
70% CRs
83% CRs

fig. S5. Eyelid PC responses during sessions with short probes. (**A**-**C**) Examples of individual eyelid PCs responses to different probe inputs. For each PC, raster plot is shown on the bottom, average firing rate, normalized to baseline, is shown for CR (blue lines) and nonCR trials (black lines). Probe trials in the raster plots are not arranged chronologically, but grouped according to the probe type (indicated on the left) and the presence or absence of behavioral response. Red dots show CR onset times. Region in grey indicates 500 ms from probe onset. (**D**) Average behavioral and eyelid PCs responses to short probes from animals trained to 1 kHz tone as a CS. Top row shows average traces of eyelid position for each probe type on CR (violet) and nonCR (black) trials. Corresponding average eyelid PCs firing rate is shown at the bottom. Region in grey indicates probe duration. Shaded regions indicate 95% confidence intervals. Independent of CR probability, the size of CRs is the same across probes. Activity of eyelid PCs on CR trials shows the same all-or-none binarity. (**E**) Data are shown in the same format as in (D), now for subjects trained with mossy fiber stimulation as CS and tested with short probes.

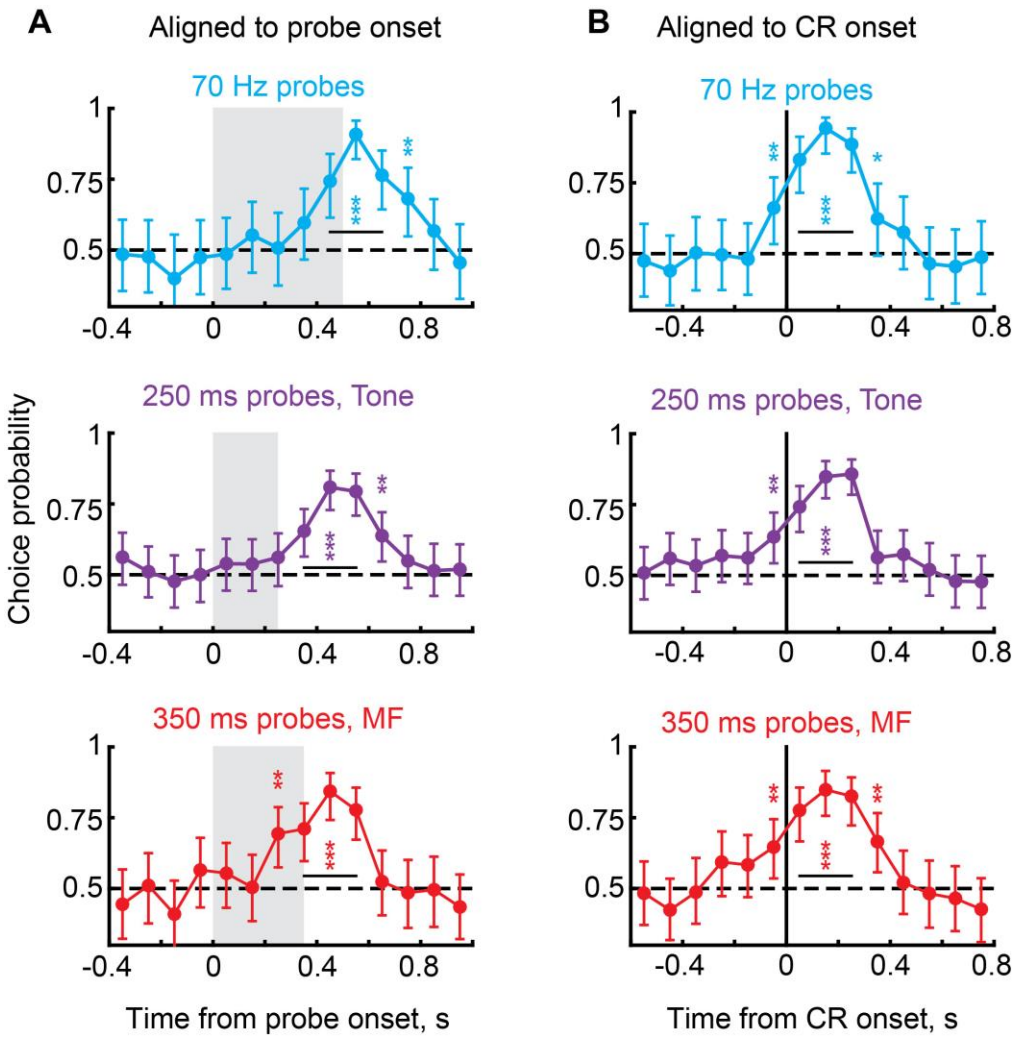

fig. S6. PC choice probabilities for individual probe types. (**A**) Layout is similar to Fig. 4 C. Choice probability as a function of time, using 100 ms non-overlapping time bins, with spike trains aligned to probe onset. A single example is shown per probe protocol: 70 Hz frequency probes (cyan), 250 ms tone short probes for subjects trained with tone as a CS (violet) and 350 ms short probes for subjects trained with mossy fiber stimulation as a CS (red). Region in grey indicates probe duration. Error-bars indicate 95% confidence intervals. Significance above chance at .05, .01 and .001 is depicted by 1, 2 or 3 stars respectively (permutation test, 5000 samples). (**B**) ROC analysis of same data, but with trials aligned by behavioral CR onset (black vertical line). In all cases, choice probability deviates above chance before behavioral CR onset. In sum, results of ROC analysis for a single probe type parallel results obtained by combining trials from several probe types (Fig. 4, C and D).

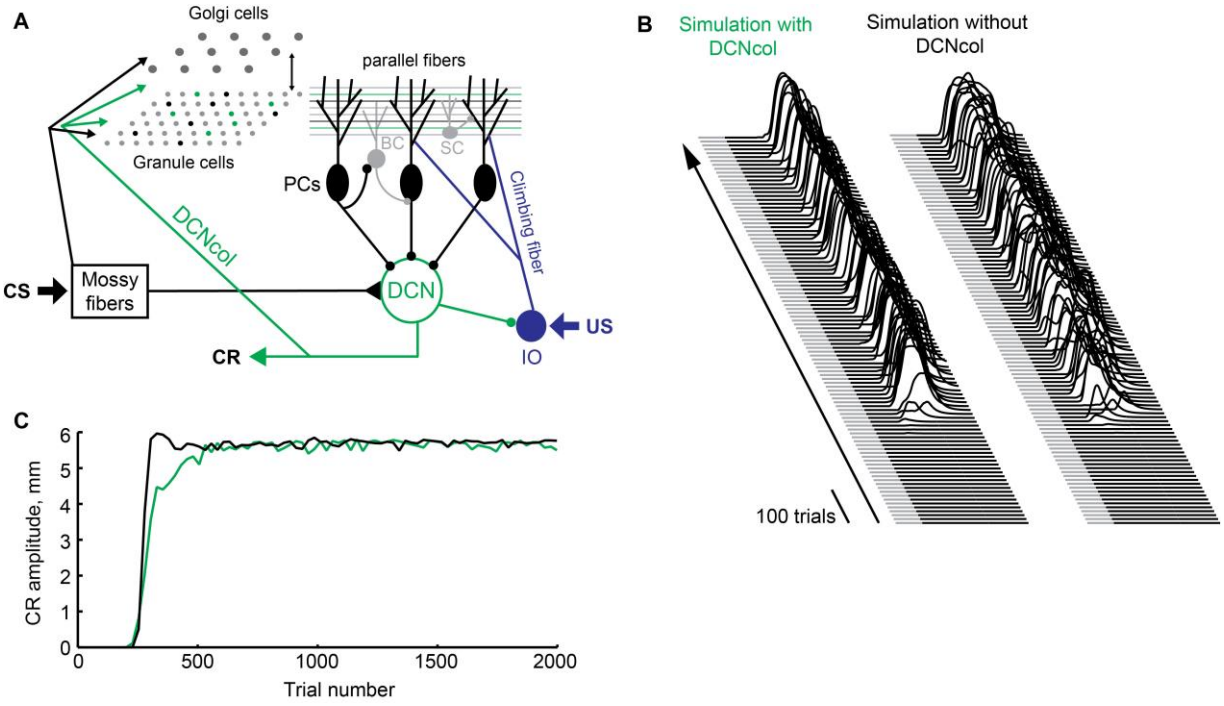

fig. S7. Acquisition of CRs in large-scale cerebellar simulations. (**A**) Schematics of cell-types in the simulation and their connectivity. (**B**) Waterfall plots of virtual eyelid position during acquisition of CRs from naïve state. Two simulations were identical except presence or absence of deep cerebellar nucleus axon collaterals (DCNcol) projecting back to the cerebellar cortex. Every 20th trial is plotted, training with Delay 500 ms protocol continued for 2000 trials. (**C**) CR amplitude as a function of trial number, averaged across blocks of 10 trials. Green line corresponds to simulation with DCNcol present, black line – without.

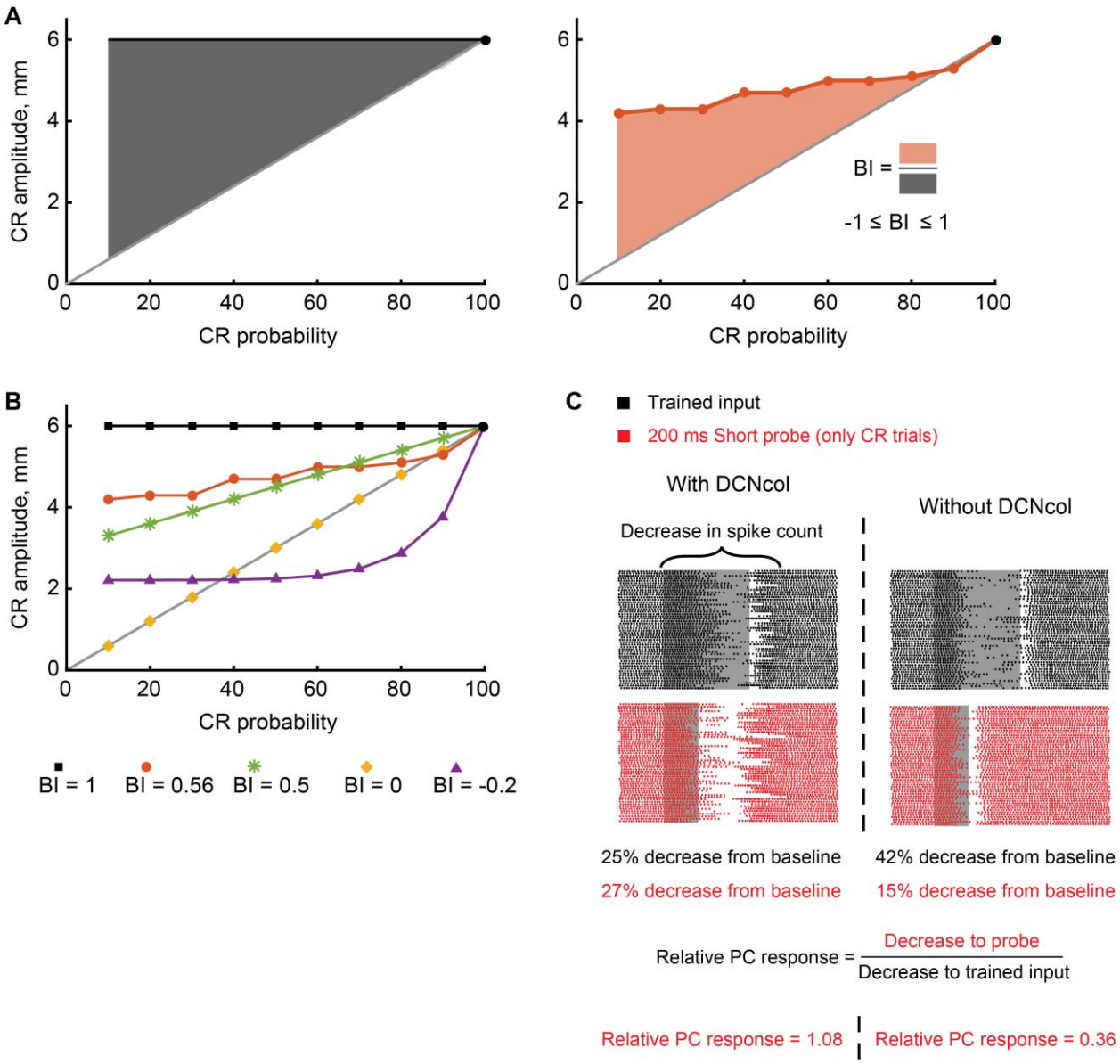

fig. S8. Definition of BI and relative PC response. (**A**) The binarity index (BI) is designed to quantify the amount of independence between CR probability and response measure (CR amplitude or PC response). Black dot represents CR amplitude and probability in response to trained stimulus. The grey diagonal line is drawn such that CR amplitude decreases at the same rate as CR probability. Black line on the left panel represents an ideal case of CR amplitude being fully independent from CR probability. Red line on the right panel illustrates a possible shape of the experimental curve. BI is calculated as ratio between red and black shaded areas. The value of BI is defined between -1 ≤ BI ≤ 1. (**B**) Five examples of possible dependence of CR amplitude on CR probability. BI = 1 corresponds to a full independence of CR amplitude from CR probability (black squares). A positive BI, but lower than one corresponds to a lower

rate of decrease in CR amplitude than in CR probability (red circles and green asterisks). BI = 0 implies a proportional scaling of CR amplitude with probability (yellow diamonds). Finally, a negative BI indicates a faster decrease in CR amplitude than in CR probability (violet triangles). (**C**) Definition of relative PC response. Scatter plots show activity of example PC from simulation with (left) or without DCNcol (right) present. PC responses to trained stimulus are shown in black, to 200 ms short probe – in red (only trials with CRs are shown). The duration of stimulus is indicated by a grey area. Notice that in simulation without DCNcol PC decrease of activity stops right after the end of probe, while in simulation with DCNcol present it persists for a similar duration as with trained stimulus. Relative PC response is defined as a ratio between reductions in PC spike count on probe trials versus trials with trained input. This way, a value close to one indicates that PC response remained the same on CR trials in response to both probe and trained stimulus.

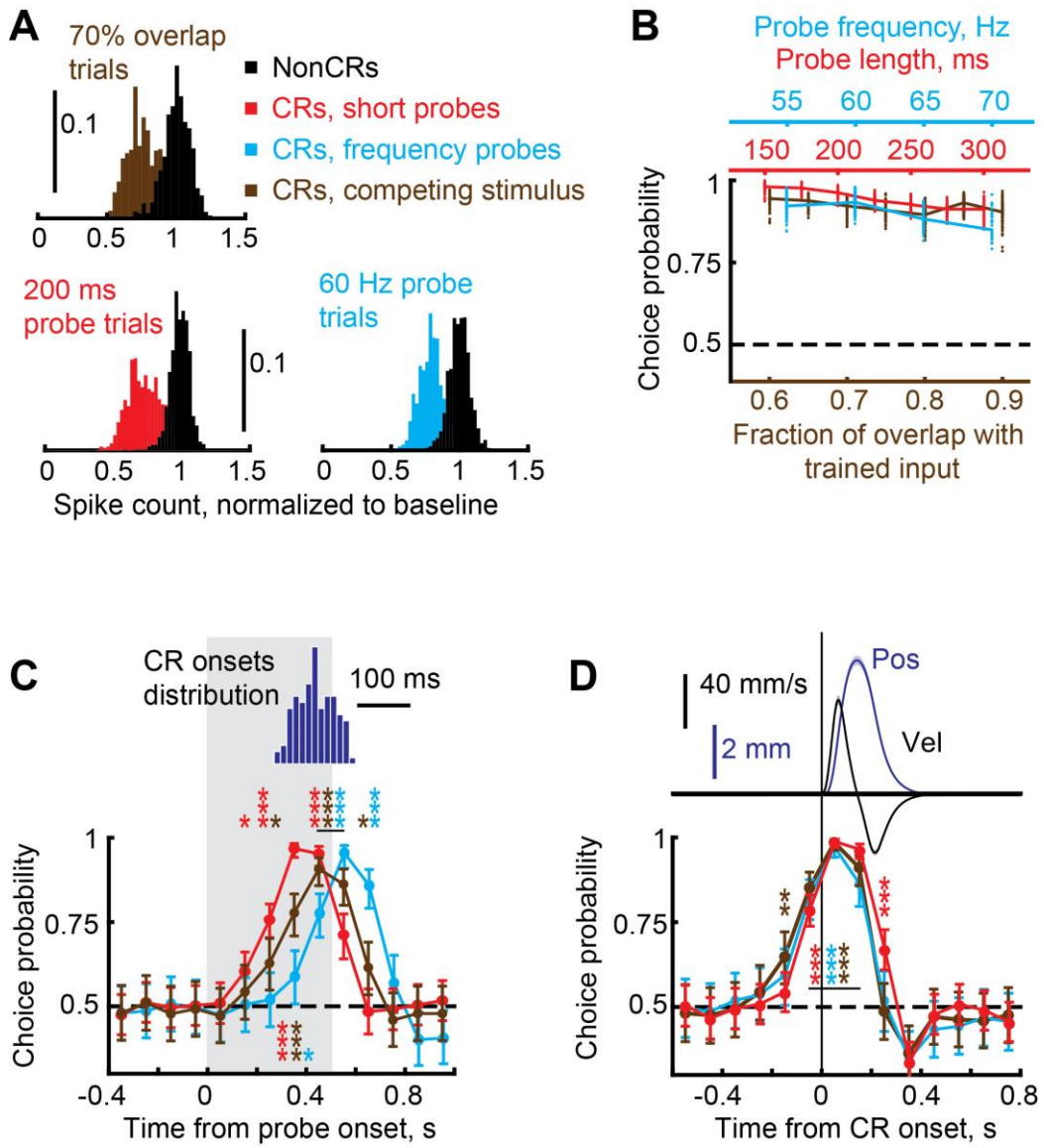

fig. S9. ROC analysis of PC activity from simulation with DCNcol. The layout is identical to Fig. 4. (**A**) Frequency distributions of PC spike counts on CR (color-coded) and non-CR trials (black). (**B**) Choice probability calculated using ROC analysis for each probe type within three probe protocols with at least 5% of CRs and nonCRs. Each dot indicates result of a random draw (100 draws are shown). Each draw determined a set of Purkinje cells and trials from which data (200 probe trials) was collected. As with recorded data, PCs choice probability was independent from probe type and CR probability. (**C**-**D**) Choice probability as a function of time, with trials aligned to either onset of probe input in (C) or onset of CR in (D). Choice probability curves were calculated from the same probe types shown in A).

table S1. Two-sample Kolmogorov-Smirnov test, comparison between CR amplitude distributions to probe and trained inputs.

Frequency probes

	50 Hz probe	60 Hz probe	70 Hz probe	80 Hz probe	90 Hz probe
All responses	$p = 3 \cdot 10^{-128}$	$p = 1 \cdot 10^{-68}$	$p = 1 \cdot 10^{-37}$	$p = 4 \cdot 10^{-13}$	$p = 0.05$
Without nonCRs	$p = 0.32$	$p = 0.07$	$p = 0.14$	$p = 0.17$	$p = 0.34$

Short probes

	50 ms probe	150 ms probe	250 ms probe	350 ms probe	450 ms probe
All responses	$p = 1 \cdot 10^{-168}$	$p = 3 \cdot 10^{-87}$	$p = 5 \cdot 10^{-30}$	$p = 3 \cdot 10^{-7}$	$p = 0.12$
Without nonCRs	$p = 0.65$	$p = 0.26$	$p = 0.051$	$p = 0.99$	$p = 0.42$

Competing stimulus

	35% overlap	50% overlap	65% overlap	80% overlap
All responses	$p = 1 \cdot 10^{-101}$	$p = 3 \cdot 10^{-77}$	$p = 1 \cdot 10^{-33}$	$p = 7 \cdot 10^{-6}$
Without nonCRs	$p = 0.11$	$p = 0.20$	$p = 0.39$	$p = 0.35$

Frequency probes, 3 mm target CR amplitude

	50 Hz probe	60 Hz probe	70 Hz probe	80 Hz probe	90 Hz probe
All responses	$p = 7 \cdot 10^{-66}$	$p = 1 \cdot 10^{-38}$	$p = 3 \cdot 10^{-22}$	$p = 5 \cdot 10^{-5}$	$p = 0.46$
Without nonCRs	$p = 0.07$	$p = 0.21$	$p = 0.03$	$p = 0.47$	$p = 0.53$

table S2. Results of two-way ANOVA on PC spike counts to different probe inputs on CR and non-CR trials. Relevant to Fig. 3 F. Results are shown separately for three probe protocols used during recordings.

	Probe type	CR/nonCR	Interaction
Frequency probes	$F_{3,414} = 0.08$ $p = 0.97$	$F_{1,414} = 152.1$ $p = 6 \cdot 10^{-30}$	$F_{3,414} = 2.25$ $p = 0.08$
Short probes, MF. stim. CS	$F_{3,468} = 0.53$ $p = 0.66$	$F_{1,468} = 58.4$ $p = 1 \cdot 10^{-13}$	$F_{3,468} = 0.66$ $p = 0.58$
Short probes, 1 kHz tone CS	$F_{4,907} = 1.33$ $p = 0.26$	$F_{1,907} = 82.5$ $p = 7 \cdot 10^{-16}$	$F_{4,907} = 1.53$ $p = 0.19$